Combustion synthesis and electrochemical properties of $LiNi_{1/3}Co_{l/3}Mn_{l/3}Br_xO_{2-x}$ and $LiNi_{1/3}Co_{l/3}Mn_{l/3}Br_xO_{2-x}$/graphene cathode material for Li-ion batteries

Jiping Zhu*, Jie Zhu, Yangyang Zhang, Juan Wang and Jiawei Yan

School of Materials Science and Engineering, Hefei University of Technology, Hefei, Anhui230009, P R China

Abstract: The layered $LiNi_{1/3}Co_{l/3}Mn_{l/3}Br_xO_{2-x}$ ($0\leq x\leq 0.09$) cathode materials were prepared by a combustion method. The XRD results indicate that the Br-doped $LiNi_{1/3}Mn_{1/3}Co_{1/3}O_2$ has the same layered structure as the pristine $LiNi_{1/3}Mn_{1/3}Co_{1/3}O_2$. FE-SEM results indicate that the particle size distribution of samples is uniform. Electrochemical tests reveal that Br-doped samples exhibit higher discharge capacity and rate capability compared with the pristine, especially the $LiNi_{1/3}Co_{l/3}Mn_{l/3}Br_{0.05}O_{1.95}$ sample shows initial discharge capacity，which can reach to 175.4 and 166.4mAh/g at 0.5 and 1.0C, respectively. Finally， an electronically conducting 2D network of graphene was introduced into $LiNi_{1/3}Co_{l/3}Mn_{l/3}Br_{0.05}O_{1.95}$ cathode material. The electrochemical properties of the materials were investigated by charge-discharge tests and electrochemical impedance spectroscopy. The charge-discharge tests demonstrate that this sample has better cycle stability than $LiNi_{1/3}Co_{l/3}Mn_{l/3}Br_{0.05}O_{1.95}$ which can be attributed to the excellent electronic conductivity and stable chemical properties of graphene. The EIS results reveal that the graphene coated greatly decreases the resistance of lithium batteries, especially the charge transfer resistance which can be attributed to the significantly improved electronic conductivity.

Key words: $LiNi_{1/3}Mn_{1/3}Co_{1/3}O_2$, Br-doping, graphene, combustion synthesis.

1. Introduction

During the past few decades, the rechargeable lithium-ion batteries (LIBs) have been one of the most important energy storage systems owing to its high energy, high energy density and good cycle performance. $LiCoO_2$ was the most commercial cathode material for LIBs due to its excellent cycle performance and relative ease of synthesis, but its application is limited because of the high price and the toxicity of cobalt. Therefore, much effort has been committed to developing $LiNi_xCo_yMn_{1-y}O_2$ layered compounds, especially for $LiNi_{1/3}Mn_{1/3}Co_{1/3}O_2$ in terms of its low cost, high discharge capacity and high thermal stability. Unfortunately, poor rate capability and fast capacity fading indeed restrict its widely application [1-4].

In order to overcome these serious problems of $LiNi_{1/3}Mn_{1/3}Co_{1/3}O_2$ material, researchers have done a lot of work. Summary previous reports, three methods are often used to improve its electrochemical performance. (1) Exploring an effective way to synthesis nanoparticles，which can shorten the diffusion distance of lithium ions and greatly increase the contact area between electrodes and electrolytes [1,5-6]. Recently, Hua et al successfully developed a fast co-precipitation method for the large scale synthesis of nanoflower structure $LiNi_{1/3}Co_{1/3}Mn_{1/3}O_2$ with the discharge capacity up to 126mAhg^{-1} at 20C when voltage range of 2.7-4.3V [5]. (2)Doping, partial cationic replace for the transition metal ions Ni, Co and Mn or anionic substitution for oxygen which can improve electronic conductivity. Such as,

Foundation item: Projects (No. 21373074) supported by the national natural science foundations of China and (No. 11010202133) supported by Anhui province science and technology plan

Corresponding author: Ji-ping ZHU; Tel:18919665197; E-mail: jpzh@ustc.edu.cn

Al^{3+}[7], Na^{+} [8], Ce^{4+} [9], Ti^{4+}[10], F^{-}[11], Y^{3+}[12], etc. (3) Surface modification, coating layer can prevent dissolution of transition metals ions into the electrolyte and side reactions between electrodes and electrolyte，enhancing the rate performance and cycle performance. Such as, CaF_2[13], TiO_2[14], Al_2O_3[15], LiF[16] and SrF_2[15].

Graphene (G) has been intensively investigated due to its excellent electronic conductivity, stable chemical properties, superior mechanical properties and high specific surface area. Recently, graphene was applied in lithium ion batteries as an ideal additive component for constructing hybrid nanostructure of LIB electrodes [18-20]. Jiang et al successfully synthesize a composite material of graphene wrapped $Li_2MnO_3 \cdot LiMO_2$, (M=Mn, Ni, Co) cathode material. Compared to the pure $Li_2MnO_3 \cdot LiMO_2$, the graphene conducting framework can efficiently alleviate the polarization of pristine $Li_2MnO_3 \cdot LiMO_2$ material leading to an outstanding enhancement in cell performance and cycling stability [19].

This paper employs a simple combustion method to synthesize Br doping LNCM material. To the best of our knowledge, this is the first time that Br doping LNCM material by combustion method. This simple method could uniformly mix the metal ions and provide more heat for the reaction [6]. Compare with combustion method, traditional solid state method needs high calcination temperature and long reaction time resulting inhomogeneous or impurity with lower capacity and poor cycling performance. Co-precipitation method needs strict control the condition of reaction and quite long reaction time which is not conducive to industrial production. Sol-gel is similar to combustion method, but combustion method does not require adjustment PH [1, 8, 21-22]. Br^{-} ion substitution for O^{2-} ion may lead to an increased electronic/ionic conductivity and improved reversible specific capacity. In addition, graphene was introduced for the best Br content of the complex, which is utilize for excellent electron conductivity and stable chemical properties of graphene.

2. Experimental

2.1 Synthesis of $LiNi_{1/3}Co_{l/3}Mn_{l/3}O_2$ with Br-doping

$LiNi_{1/3}Co_{l/3}Mn_{l/3}O_2$ material was synthesized by combustion method using tartaric acid as combustion agent. Firstly, the stoichiometric amounts of lithium acetate (5% excess amount of lithium acetate was used to compensate Li loss during the calcination), nickel acetate, cobalt acetate and manganese acetate were dissolved in ethylene glycol. In addition, the molar ratio of the tartaric acid to metal ions was 1:1. Secondly, the mixed solution was under magnetic stirring at 25℃for 1h and then was heated at 150℃ for 6h. Thirdly, the obtained mixture was ground and then put into an Al_2O_3 crucible. The crucible was put in a muffle furnace preheated at 450℃ for 6 h in air to eliminate the organic composition and then was sintered at 850℃ for 10h. The sample heating rate of 4℃min^{-1} and then slowly cooled to room temperature.

In order to obtain the Br-doped samples, the same procedures were carried out, only at the beginning adding lithium bromide. $LiNi_{1/3}Co_{l/3}Mn_{l/3}Br_xO_{2-x}$ (x=0.01, 0.03, 0.05, 0.07, 0.09) samples were gained by adjusting the content of LiBr.

2.2 Synthesis of $LiNi_{1/3}Co_{l/3}Mn_{l/3}Br_{0.05}O_{1.95}$/G composite

Graphite oxide (GO) nanosheets were fabricated via a modified Hummers method using natural graphite powders as the raw material. 2.0g/L graphene oxide solution was prepared by graphite oxide powder dissolve into ethanol solution followed by ultrasonication for 0.5h. Meanwhile, the previous synthesis $LiNi_{1/3}Co_{l/3}Mn_{l/3}Br_{0.05}O_{1.95}$ was dissolved into ethanol solution and vigorously stirred for 30min. Then, the previously prepared GO solution was added into the $LiNi_{1/3}Co_{l/3}Mn_{l/3}Br_{0.05}O_{1.95}$ suspension with 3wt% content of GO. Subsequently, the mixed solution was transferred to a Teflon-lined autoclave at 120℃for 3h. As the end of reaction, the products were filtered and washed using distilled water and ethanol several times, then dried at 65℃in an oven.

2.3 Material characterization and electrochemical measurements

The crystalline structure of the samples was analyzed by an X-ray diffraction (XRD, X'Pert PRO MPD) measurements using Cu Kα radiation. The scan data was recorded in the 2θ range of 10–80°. The field-emission scanning electron microscope (FE-SEM, SU8020)

equipped with an energy dispersive spectroscope (EDS) was used to study the morphologies and elements distribution of samples. The powder was dispersed into ethanol and a drop of the suspension was transferred onto aluminum foil and dried for FE-SEM observations.

The electrochemical performance of the as-synthesized material was investigated in CR2032 coin cells. The coin cell contained a test electrode (cathode), a pure lithium foil (anode), a microporous polyethylene membrane, and an electrolyte solution. For the test electrode, a mixture of active material, acetylene black, and polyvinylidene fluoride (PVDF) binder at a weight ratio of 8:1:1 was dispersed in a N-methylpyrrolidone (NMP) solution. The slurry was paste on an aluminum foil, and dried at 120℃ for 12h in a vacuum oven. The pure lithium foil was used as a reference and counter electrode, the microporous polyethylene membrane (Celgard 2400) was used as a separator, and the electrolyte was 1 M $LiPF_6$ in a 1:1 (v/v) mixture of ethylene carbonate (EC) and diethyl carbonate (DEC). The cells were assembled in an argon-filled glove box, afterwards aged for 12 h before electrochemical test. The electrochemical impedance spectroscopy EIS) was performed on CHI660D electrochemical workstation .The frequency range was from 0.01Hz to 100k Hz and amplitude voltage was 5 mV.

3. Results and discussion

3.1 The effect of Br-doping on crystal structure, morphology and electrochemical performance

Fig. 1 illustrated the XRD patterns of the pristine and Br-doping $LiNi_{1/3}Co_{1/3}Mn_{1/3}O_2$ cathode materials. All the observed diffraction peaks are well indexed in the R-3m space with α-$NaFeO_2$ layered structure. No impurity peaks were observed, which indicated that the Br-doping does not change on the crystalline structure. The peak intensity ratio of (003)/(104) is sensitive to the degree of cation mixing in the layered compounds, and the larger I(003)/I(104) value, the less cation mixing between Li and Ni ions. A higher value (>1.2) of I(003)/I(104) is generally believed that have less cation mixing and better hexagonal structure in the layered compounds [3]. The I(003)/I(104)values of all samples are larger than 1.2, it was suggested that less cation mixing takes place. In addition, the pairs of (006)/(102) and (108)/(110) are spilt, which is considered to be the characteristic of the layered structure. It is clear that split of the (006)/(102) and (108)/(110) peaks when the doping amount of Br is less than 5%. When the content of Br doping continues to increase, the peaks split are not obvious. This phenomenon may be due to the fact that excess Br-doping decreasing crystallization of the material and it is not conducive to form stable layered structure.

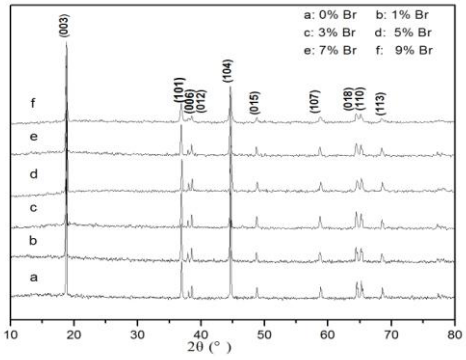

Fig.1 XRD patterns of $LiNi_{1/3}Co_{1/3}Mn_{1/3}Br_xO_{2-x}$ (x=0, 0.01, 0.03, 0.05, 0.07, 0.09)

FE-SEM images of the pristine and $LiNi_{1/3}Co_{1/3}Mn_{1/3}Br_{0.05}O_{1.95}$ are shown in Fig. 2. The pristine and Br-doping are composed of small particles with smooth surface and particle size in the range of 300nm-500nm. Compared with the pristine, the $LiNi_{1/3}Co_{1/3}Mn_{1/3}Br_{0.05}O_{1.95}$ has more homogeneous particle-size distributions, which is beneficial to intercalation and de-intercalation of lithium ions. It may bring about good electrochemical performance. Furthermore, in order to prove the homogeneity of the $LiNi_{1/3}Co_{1/3}Mn_{1/3}O_2$, the EDS results are shown in Fig.3. The results shows that transition metal elements and oxygen are homogeneously distribution on the surface of particle, and the results agreed with the XRD results, further demonstrating that the final product was $LiNi_{1/3}Co_{1/3}Mn_{1/3}O_2$.

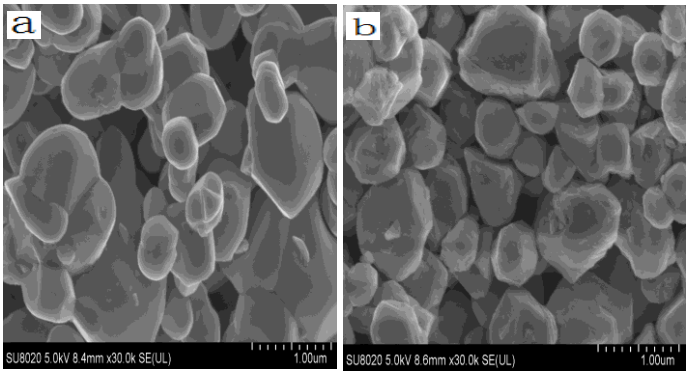

Fig.2 FE-SEM images of $LiNi_{1/3}Co_{1/3}Mn_{1/3}Br_xO_{2-x}$ (x=0, 0.03) (a) x=0, (b) x=0.03

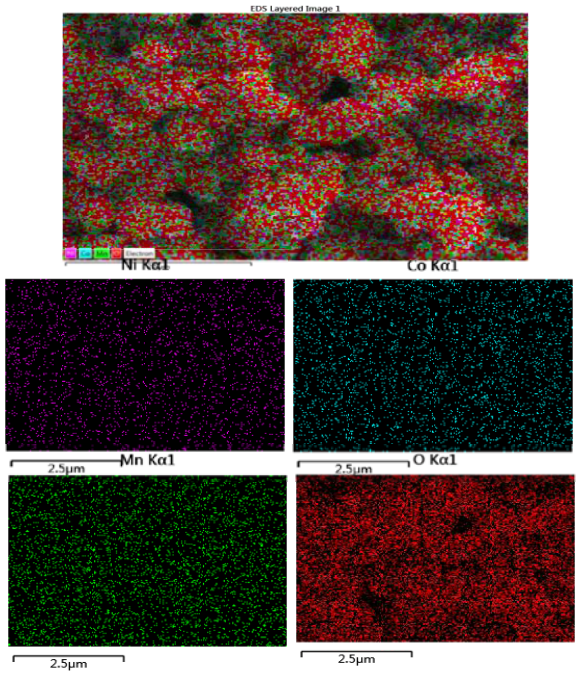

Fig.3 EDS element mapping of $LiNi_{1/3}Co_{1/3}Mn_{1/3}O_2$

The initial charge–discharge curves of the prepared $LiNi_{1/3}Co_{1/3}Mn_{1/3}Br_xO_{2-x}$ (x=0, 0.01, 0.03, 0.05, 0.07, 0.09) shown in Fig. 4 between 2.5 and 4.3 V at 0.2 C. Charge tests were performed using a constant current follow by constant voltage charge, which means charging continued at 4.3V at a constant current (0.2C), and then kept at the voltage of 4.3V until the current dropped to less than 0.02C, and then discharged to 2.5V cut-off potential in constant current. As can be seen from Fig. 4, the initial specific discharge capacities of $LiNi_{1/3}Co_{1/3}Mn_{1/3}Br_xO_{2-x}$ (x= 0, 0.01, 0.03, 0.05, 0.07, 0.09) are 157.4, 169.9, 173.7, 179.6, 156.1and 147.8mAh/g, respectively. The initial discharge capacity increased dramatically when the Br content of x is less than or equal to 0.05. The likely reason was the O^{2-} ion (0.14nm) substituted by Br^- ion (0.196nm) lead to the lattice parameter increase, which in turn may lead to an increased electronic/ionic conductivity and improved reversible specific capacity. The discharge capacity decreased when the content of Br doping continues to increase. It was suggested the excess Br-doping caused the structural instability and deteriorated of the electrochemical performance.

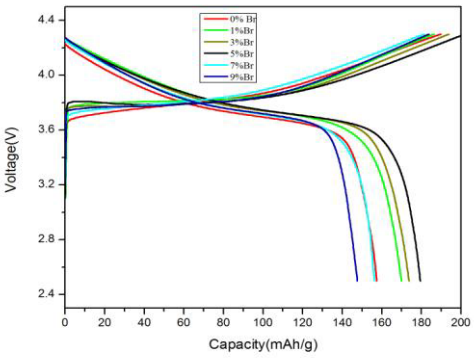

Fig.4 Initial charge/discharge curves of $LiNi_{1/3}Co_{1/3}Mn_{1/3}Br_xO_{2-x}$ (x=0, 0.01, 0.03, 0.05, 0.07, 0.09) samples at 0.2C

Fig. 5 showed the rate capacity of the pristine and $LiNi_{1/3}Co_{1/3}Mn_{1/3}Br_{0.05}O_{1.95}$ samples. The cells were charged to 4.3V at the current 0.1C, and then discharged to 2.5V at 0.2, 0.5, 1.0 and 2.0 C, respectively. Obviously, with the increase of current density, the discharge capacity of the two samples reduced gradually. Moreover, the $LiNi_{1/3}Co_{1/3}Mn_{1/3}Br_{0.05}O_{1.95}$ sample delivers higher capacity than the pristine at the same currents. The $LiNi_{1/3}Co_{1/3}Mn_{1/3}Br_{0.05}O_{1.95}$ sample shows a high discharge capacity of 175.4, 166.4 and 153.9mAh/g at 0.5, 1.0 and 2.0C, remaining 97.6%, 92.6%and 87.7% of the capacity of 179.6mAh/g at the 0.2 C. The improved rate capacity of the $LiNi_{1/3}Co_{1/3}Mn_{1/3}Br_{0.05}O_{1.95}$ sample can be partially ascribed to the increased electronic/ionic conductivity due to Br-doping.

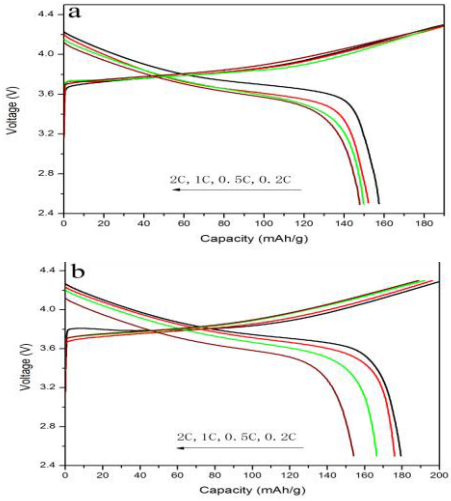

Fig.5 Rate capacity of (a) $LiNi_{1/3}Co_{1/3}Mn_{1/3}O_2$ and (b) $LiNi_{1/3}Co_{1/3}Mn_{1/3}Br_{0.05}O_{1.95}$ samples

Cycling performance of the pristine and $LiNi_{1/3}Co_{1/3}Mn_{1/3}Br_{0.05}O_{1.95}$ are shown in Fig. 6. In both cases, the specific capacities decreased gradually during cycles, which may be attributed to the corrosion of the electrode by the electrolytes. After 50 charge/discharge cycles, the specific discharge capacity of $LiNi_{1/3}Co_{1/3}Mn_{1/3}Br_{0.05}O_{1.95}$ sample is 133.1mAh/g, however, its retention rate is lower than the pristine, which the pristine retained around 78.8% of the initial discharge capacity. The $LiNi_{1/3}Co_{1/3}Mn_{1/3}Br_{0.05}O_{1.95}$ sample suffered a severe capacity fading, which may be lead to transition ions easily dissolved in the electrolyte caused by Br doping.

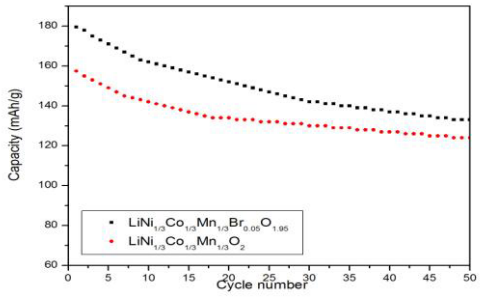

Fig.6 Cycling performance of $LiNi_{1/3}Co_{1/3}Mn_{1/3}O_2$ and $LiNi_{1/3}Co_{1/3}Mn_{1/3}Br_{0.05}O_{1.95}$ samples at 0.2C

3.2 Crystal structure, morphology and electrochemical performance of $LiNi_{1/3}Co_{1/3}Mn_{1/3}Br_{0.05}O_{1.95}$/G sample

Recent advances show that graphene can serve as a perfect 2D support on the edges and surface for anchoring metal or metal oxide nanoparticles [17-18, 23]. GO was fabricated via a modified Hummers method contain many hydrophilic oxygen-containing functional groups, such as –COOH, -OH, C=O and epoxy groups, which enables GO to be well dispersed [25]. Solvothermal method is considered to be an effective and practical method for producing graphene/metal oxide composite materials. In order to further prove solvothermal method is involved in the reduction of GO to G. XRD patterns of the GO and G samples are show in Fig.7 (a). The XRD patterns of the $LiNi_{1/3}Co_{1/3}Mn_{1/3}Br_{0.05}O_{1.95}$ and $LiNi_{1/3}Co_{1/3}Mn_{1/3}Br_{0.05}O_{1.95}$/G are depicted in Fig.7(b) . All diffraction peaks can be indexed in the R-3m space with α-$NaFeO_2$ structure. All samples showing a typical hexagonal layered structure because the (006)/(102) and (108)/(110) peaks are well separated. In addition, graphene characteristic XRD peaks not being detected in the XRD pattern, this may be due to the low content of graphene.

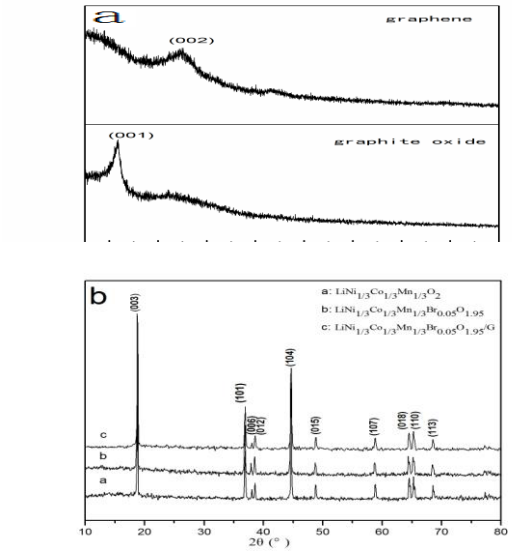

Fig.7 XRD patterns of (a) graphite oxide and graphene (b)$LiNi_{1/3}Co_{1/3}Mn_{1/3}O_2$, $LiNi_{1/3}Co_{1/3}Mn_{1/3}Br_{0.05}O_{1.95}$, $LiNi_{1/3}Co_{1/3}Mn_{1/3}Br_{0.05}O_{1.95}$/G

Fig.8 shows the FE-SEM images of the $LiNi_{1/3}Co_{1/3}Mn_{1/3}Br_{0.05}O_{1.95}$/*G* composites at different magnifications. Graphene sheets are uniformly distributed among the $LiNi_{1/3}Co_{1/3}Mn_{1/3}Br_{0.05}O_{1.95}$ particles, giving a better connection between adjacent $LiNi_{1/3}Co_{1/3}Mn_{1/3}Br_{0.05}O_{1.95}$ particles, as well as preventing them from further aggregation. In addition, the presence of

graphene may be inhibit the dissolution of metal ions and increase electronic/ionic conductivities, which is of great importance in improving electrochemical performance.

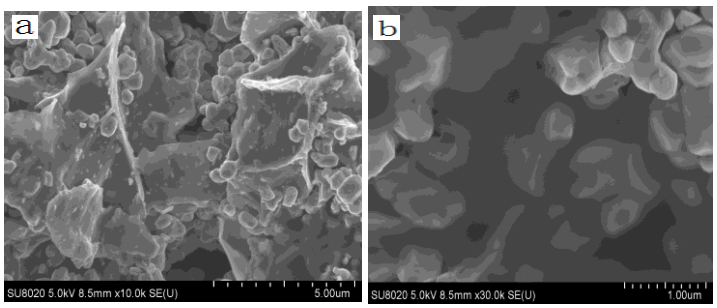

Fig.8 FE-SEM images of $LiNi_{1/3}Co_{1/3}Mn_{1/3}Br_{0.05}O_{1.95}$/G

The initial charge–discharge curves of the $LiNi_{1/3}Co_{1/3}Mn_{1/3}Br_{0.05}O_{1.95}$ and $LiNi_{1/3}Co_{1/3}Mn_{1/3}Br_{0.5}O_{1.95}$/G are shown in Fig. 9. Both samples clearly displayed a potential plateau around 3.6–3.8 V during the charge-discharge processes, which in agreement with typical layer structured $LiNi_{1/3}Co_{1/3}Mn_{1/3}O_2$ reported by many researchers [4, 20]. The specific discharge capacities of the $LiNi_{1/3}Co_{1/3}Mn_{1/3}Br_{0.05}O_{1.95}$ and $LiNi_{1/3}Co_{1/3}Mn_{1/3}Br_{0.5}O_{1.95}$/G are 179.6 and 181.3 mAh/g at 0.2C, respectively. Both samples of the first discharge specific capacity is very similar, but their cycle performance difference, as shown in Fig. 10. It is clear that the discharge capacity of the graphene coated reach to 145mAh/g after 50 cycles, higher than that of the $LiNi_{1/3}Co_{1/3}Mn_{1/3}Br_{0.05}O_{1.95}$ sample at 133.1mAh/g. One possible reason is that the graphene coated stabilizes the surface structure of the layered oxide, thereby reduced the dissolution of metal ions.

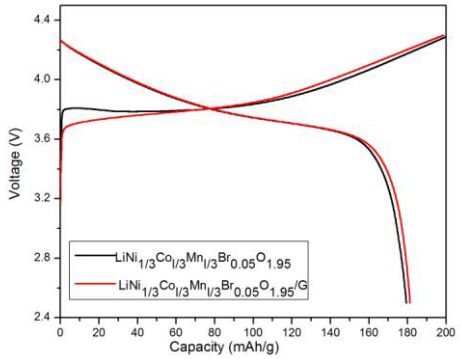

Fig.9 Initial charge/discharge curves of $LiNi_{1/3}Co_{1/3}Mn_{1/3}Br_{0.5}O_{1.95}$ and $LiNi_{1/3}Co_{1/3}Mn_{1/3}Br_{0.5}O_{1.95}$ /G samples at 0.2C

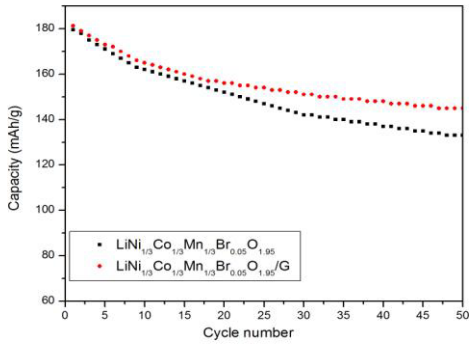

Fig.10 Cycling performance of $LiNi_{1/3}Co_{1/3}Mn_{1/3}Br_{0.05}O_{1.95}$ and $LiNi_{1/3}Co_{1/3}Mn_{1/3}Br_{0.5}O_{1.95}$/G samples at 0.2C

The electrochemical impedance spectra (EIS) of the $LiNi_{1/3}Co_{1/3}Mn_{1/3}Br_{0.05}O_{1.95}$ and $LiNi_{1/3}Co_{1/3}Mn_{1/3}Br_{0.5}O_{1.95}$/G electrodes are shown Fig. 11. The impedance spectra exhibit two semicircles in the high and intermediate-frequency ranges and followed by a straight slopping line in the low frequency region. The high frequency semicircle is related the Li^+ ion migration resistance (R_{sei}) through the solid electrolyte interface (SEI) film that forms on the surface of the cathode materials; the intermediate frequency semicircle is attributed to the charge transfer resistance (R_{ct}) in the cathode/electrolyte interface; the low frequency tail is attribute to Warburg impedance that is associated with Li^+ diffusion through the cathode [25-28]. From the Fig.11, it could also see that the first semicircle has virtually no change of these two samples, which means the solid electrolyte interface layer formed on the surface of the electrode has no great difference. However, the R_{ct} of $LiNi_{1/3}Co_{1/3}Mn_{1/3}Br_{0.05}O_{1.95}$/G sample is significantly smaller than that of $LiNi_{1/3}Co_{1/3}Mn_{1/3}Br_{0.05}O_{1.95}$. One interpretation is that it is the graphene coated improved electronic conductivity and stabilizes the surface structure of the layered oxide, thus the dissolution of metal ions is reduced. Small impedance is conducive to the intercalation and de-intercalation of lithium-ions during the charge and discharge process. Hence, the EIS test also can confirm the improvement of electrochemical properties.

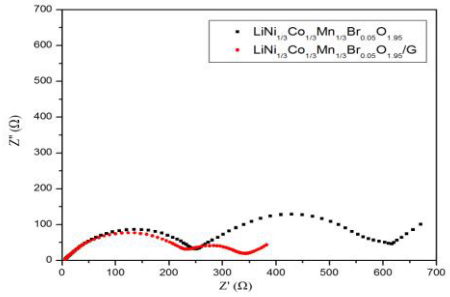

Fig.11 Electrochemical impedance spectra of $LiNi_{1/3}Co_{1/3}Mn_{1/3}Br_{0.05}O_{1.95}$ and $LiNi_{1/3}Co_{1/3}Mn_{1/3}Br_{0.5}O_{1.95}$ /G samples

4. Conclusions

Layered-structured $LiNi_{1/3}Co_{1/3}Mn_{1/3}Br_xO_{2-x}$ ($0 \le x \le 0.08$) materials were successful synthesized by combustion method. The structure, morphology and electrochemical properties of samples were investigated in detail. The results show that Br-doping does not alter the structure of $LiNi_{1/3}Mn_{1/3}Co_{1/3}O_2$, and exhibits higher discharge capacity, better cycle performance and rate capability. Particularly the $LiNi_{1/3}Co_{1/3}Mn_{1/3}Br_{0.05}O_{1.95}$ sample shows a discharge capacity of 179.6, 175.4, 166.4 and 153.9mAh/g at 0.2, 0.5, 1.0 and 2.0C, respectively. Finally, graphene was introduced to the composite through a simple solvothermal method. The cycle performance of $LiNi_{1/3}Co_{1/3}Mn_{1/3}Br_{0.05}O_{1.95}$/G (3wt%) composites are much better than $LiNi_{1/3}Co_{1/3}Mn_{1/3}Br_{0.05}O_{1.95}$. EIS results reveal that graphene modification improved electronic conductivity and reduce the charge transfer impedance of material.

References

[1] F.Wu, M. Wang, Y.f. Su, A novel method for synthesis of layered $LiNi_{1/3}Mn_{1/3}Co_{1/3}O_2$ as cathode material for lithium-ion battery, J. Power Sources, **195** (2010)

[2] C.X. Ding, Y.C. Bai, X.Y. Feng, Improvement of electrochemical properties of layered $LiNi_{1/3}Co_{1/3}Mn_{1/3}O_2$ positive electrode material by zirconium doping, Solid State Ionics, **189** (2011)

[3] X.Z Liu, P. He, H.Q Li, Improvement of electrochemical properties of $LiNi_{1/3}Co_{1/3}Mn_{1/3}O_2$ by coating with V_2O_5 layer, J.Alloys Compd., **552** (2013)

[4] P. Robert Ilango, T. Subburaj, K. Prasanna, Physical and electrochemical performance of $LiNi_{1/3}Co_{1/3}Mn_{1/3}O_2$ cathodes coated by Sb_2O_3 using a sol-gel process, Mater. Chem. Phys., **158** (2015)

[5] W.B. Hua, X.D. Guo, Z. Zheng, Uncovering a facile large-scale synthesis of $LiNi_{1/3}Co_{1/3}Mn_{1/3}O_2$ nanoflowers for high power lithium-ion batteries, J. Power Sources, **275** (2015)

[6] J.L. Zheng, W. Zhou, Y.R. Ma, Combustion synthesis of $LiNi_{1/3}Co_{1/3}Mn_{1/3}O_2$ powders with enhanced electrochemical performance in LIBs, J.Alloys Compd., **635** (2015)

[7] Y.H.Ding, P. Zhang, Z.L. Long, Morphology and electrochemical properties of Al doped $LiNi_{1/3}Co_{1/3}Mn_{1/3}O_2$ nanofibers prepared by electrospinning, J.Alloys Compd., **487** (2009)

[8] C.X. Gong, W.X. Lv, L.M. Qu, Syntheses and electrochemical properties of layered $Li_{0.95}Na_{0.05}Ni_{1/3}Co_{1/3}Mn_{1/3}O_2$ and $LiNi_{1/3}Co_{1/3}Mn_{1/3}O_2$, J. Power Sources, **247** (2014)

[9] S.K.Zhong, Y.Wang, J.Q.Liu, Synthesis and electrochemical properties of Ce-doped $LiNi_{1/3}Mn_{1/3}Co_{1/3}O_2$ cathode material for Li-ion batteries,J. rare earths, **299**(2011).

[10] G.Y Li, Z.L. Huang, Z.L. Zuo, Understanding the trace Ti surface doping on promoting the low temperature performance of $LiNi_{1/3}Co_{1/3}Mn_{1/3}O_2$ cathode, J. Power Sources, **281** (2015)

[11] Masaya Kageyama, Decheng Li, Koichi Kobayakawa, Structural and electrochemical properties of $LiNi_{1/3}Mn_{1/3}Co_{1/3}O_{2-x}F_x$ prepared by solid state reaction, J. Power Sources, **157** (2006)

[12] Y.W Li, Y.X. Li, S.K. Zhong, Synthesis and Electrochemical Properties of Y-Doped $LiNi_{1/3}Co_{1/3}Mn_{1/3}O_2$ Cathode Materials for Li-Ion Battery, Integrated Ferroelectrics, **127**(2011)

[13] Ke Xua, Zhifu Jie a,b, Ronghua Li, Synthesis and electrochemical properties of CaF_2-coated for long-cycling $Li[Mn_{1/3}Co_{1/3}Ni_{1/3}]O_2$ cathode materials, Electrochimica Acta, **60** (2012)

[14] F.Wu, M. Wang, Y.f. Su, Effect of TiO_2-coating on the electrochemical performances of $LiNi_{1/3}Co_{1/3}Mn_{1/3}O_2$, J. Power Sources, **191** (2009)

[15] X.L Li, W.X. He, L. Chen, Hydrothermal synthesis and electrochemical performance studies of

Al_2O_3-coated $LiNi_{1/3}Co_{1/3}Mn_{1/3}O_2$ for lithium-ion batteries, Ionics, **20** (2014)

[16] S.J. Shi, J.P. Tu, Y.Y. Tang, Enhanced electrochemical performance of LiF-modified $LiNi_{1/3}Co_{1/3}Mn_{1/3}O_2$ cathode materials for Li-ion batteries, J. Power Sources, **225** (2013)

[17] J.G. Li, L. Wang, Q. Zhang, Electrochemical performance of SrF_2-coated $LiNi_{1/3}Co_{1/3}Mn_{1/3}O_2$ cathode materials for Li-ion batteries, J. Power Sources, **190** (2009)

[18] Z.S. Wu, G.M. Zhou, L.C. Yin, Graphene/metal oxide composite electrode materials for energy storage, Nano Energy, **1** (2012)

[19] K.C. Jiang, X.L. Wu, Y.X. Yin, Superior Hybrid Cathode Material Containing Lithium-Excess Layered Material and Graphene for Lithium-Ion Batteries, ACS Applied Materials & Interfaces, **49** (2012)

[20] K.C. Jiang, S Xin, J.S. Lee, Improved kinetics of $LiNi_{1/3}Mn_{1/3}Co_{1/3}O_2$ cathode material through reduced graphene oxide networks, Phys. Chem. Chem. Phys., **14** (2012)

[21] C. Deng, S. Zhang, L. Ma, Effects of precipitator on the morphological, structural and electrochemical characteristics of $Li[Ni_{1/3}Co_{1/3}Mn_{1/3}]O_2$ prepared via carbonate coprecipitation, J.Alloys Compd., **509** (2011)

[22] P. Gao, G. Yang, H.D. Liu, Lithium diffusion behavior and improved high rate capacity of $LiNi_{1/3}Co_{1/3}Mn_{1/3}O_2$ as cathode material for lithium batteries, Solid State Ionics,**207** (2012)

[23] I.V. Lightcap, T.H. Kosel, P.V. Kamat, Anchoring Semiconductor and Metal Nanoparticles on a Two-Dimensional Catalyst Mat.Storing and Shuttling Electrons with Reduced Graphene Oxide, Nano Letters, **10** (2010)

[24] Gints Kucinskis, Gunars Bajars, Janis Kleperis,Graphene in lithium ion battery cathode materials: A review, J. Power Sources, **240** (2013)

[25] F.Wu, M. Wang, Y.f. Su, A novel layered material of $LiNi_{0.32}Mn_{0.33}Co_{0.33}Al_{0.01}O_2$ for advanced lithium-ion batteries, J. Power Sources **195** (2010)

[26] Y.Y. Hu, Y.K. Zhou, J. Wang, Preparation and characterization of macroporous $LiNi_{1/3}Co_{1/3}Mn_{1/3}O_2$ using carbon sphere as template, Mater. Chem. Phys. **129** (2011)

[27] G.T.-K. Fey, P. Muralidharan, C.-Z. Lu, Y.-D. Cho, Enhanced electrochemical performance and thermal stability of La_2O_3-coated $LiCoO_2$, Electrochim Acta, **51 (**2006)

[28] Z.R. Zhang, H.S. Liu, Z.L Gong, Electrochemical performance and spectroscopic characterization of TiO_2-coated $LiNi_{0.8}Co_{0.2}O_2$ cathode materials, J. Power Sources, **129** (2004)